ELSEVIER

Chemical Engineering Journal 87 (2002) 73–88

Chemical Engineering Journal

www.elsevier.com/locate/cej

Mathematical modelling of Claus reactors undergoing sulfur condensation and evaporation

A.N. Zagoruiko*, Yu.Sh. Matros[1]

Boreskov Institute of Catalysis, Pr. Akad. Lavrentieva 5, 630090 Novosibirsk, Russia

Received 5 February 2001; accepted 23 July 2001

Abstract

The paper is dedicated to the mathematical modelling of Claus reaction performance in the packed catalyst bed under conditions of sulfur condensation and evaporation. The proposed mathematical model accounts for heat and mass transfer between reaction gas and solid catalyst, condensation and evaporation of sulfur, reversible catalyst deactivation by liquid sulfur, Claus reaction reversibility, intraparticle diffusion limitations, heat conductivity of the catalyst bed frame. Reverse-flow operation of the catalyst bed have been investigated. The complex process flow-sheets, comprising two and three catalyst beds with intermediate sulfur condensers, have been simulated. It has been shown, that application of the reverse-flow technique provides increase of process efficiency.

Keywords: Sulfur; Hydrogen sulphide; Claus process; Reverse-flow operation; Sulfur condensation; Mathematical modelling

1. Introduction

Recovery of elemental sulfur from industrial waste gases is an important problem both from environmental and economic points of view. On one hand, the rise of sulfur volumes in waste gases together with tightening emission regulations leads to the increase of recovered sulfur production. From the other hand, the tightening of sulfur market imposes harder requirements to cost of produced sulfur. From this point of view, the development of new highly efficient and low cost production sulfur technologies is worthy.

The major source of recovered sulfur is hydrogen sulphide, mainly produced as a by-product at natural gas processing plants and oil refineries. First method of H_2S treatment, based on oxidation of hydrogen sulphide into sulfur by oxygen

$$H_2S + \tfrac{1}{2}O_2 \Rightarrow \tfrac{1}{n}S_n + H_2O \quad (1)$$

in the packed bed of bauxite catalyst, was proposed by C.F. Claus more than a century ago [1–3]. The said process was significantly improved in 1930s by IG Farbenidustrie [4,5], who proposed to perform preliminary homogeneous oxidation of H_2S by oxygen in a furnace with following catalytic interaction of unreacted H_2S and formed SO_2:

$$H_2S + \frac{1}{2}SO_2 \Rightarrow \frac{1.5}{n}S_n + H_2O \quad (2)$$

in separate catalytic reactors. Reaction (2) is now called Claus reaction and the proposed process is called Claus process, though they both actually do not have any relation to the inventions of C.F. Claus. At the moment the Claus technology is used in industry in hundreds of plants world-wide. Usually, the catalysts, based on γ-Al_2O_3 or TiO_2, are applied in the process.

The Claus reaction is exothermic (below $\sim$550 °C) and reversible, so the minimum reaction temperature is required to provide favourable thermodynamic conditions for maximum conversion. At the same time the decrease of temperature is limited by the sulfur dew point. Reaction performance below this limit leads to sulfur condensation in the catalyst bed, leading to the blockade of catalyst surface and its deactivation. Thus, to achieve high conversion the process is usually performed in two or three consecutive catalytic reactors with intermediate removal of sulfur in condensers [6]. The conventional two-stage system (see Fig. 1a) provides the degree of sulfur recovery of up to 96%, and the three-stage one up to 98% [7]. Obviously, the presence of few reactors and a lot of heat-exchanging devices lead to cumbersome and relatively expensive plants.

Further increase of sulfur recovery degree (up to 99.9% and even higher) may be achieved by application of additional Claus tail-gas cleanup processes. Among variety of such technologies the following three groups of such

* Corresponding author. Tel.: +7-3832-344491; fax: +7-3832-341878.
E-mail address: zagor@catalysis.nsk.su (A.N. Zagoruiko).
[1] Present address: Matros Technologies Co., Saint Louis, USA.

1385-8947/02/$ – see front matter
PII: S1385-8947(01)00203-0

Nomenclature

a	relative capacity of the catalyst pellet for liquid sulfur (see Eq. (11))
C_c	intrinsic heat capacity of the catalyst bed (kJ m^{-3} K^{-1} s^{-1})
C_i	heat capacity of ith reaction mixture component (kJ st. m^{-3} K^{-1} s^{-1})
C_p	heat capacity of reaction mixture (kJ st. m^{-3} K^{-1} s^{-1})
C_S	heat capacity of liquid (with superscript L) and gaseous (superscript G) sulfur (kJ st. m^{-3} K^{-1} s^{-1})
d	equivalent diameter of the catalyst pellet (m)
D_{eff}	effective diffusion coefficient (m^2 s^{-1})
D_{kn}	coefficient of Knudsen diffusion (m^2 s^{-1})
D_{mol}	coefficient of molecular diffusion (m^2 s^{-1})
d_p	average pore diameter in the catalyst pellet (m)
E_a	reaction activation energy (kJ mol^{-1})
f	heat-exchange factor
F	heat-exchange surface area in the heat-exchanger (m^2)
H_G	enthalpy of the reaction mixture (kJ st. m^{-3})
H_i	enthalpy of the ith substance (kJ st. m^{-3})
I	substance index
K_0	pre-exponent of kinetic constant K_1 (s^{-1})
K_1	kinetic constant in the Claus rate Eq. (27) (s^{-1})
K_2	coefficient in the Claus rate Eq. (27)
K_p	Claus reaction equilibrium constant
ℓ	axial co-ordinate (along the bed length) (m)
L	catalyst bed length (m)
m	reaction rate order
n	number of sulfur atoms in average sulfur molecule
P_i, $\hat{P}_i$	partial pressure (concentration) of ith substance (volume fraction = st. m^3) of the substance per cubic meter of the bed) in the gas flow and near the catalyst surface, respectively
P^*	equilibrium partial pressures (concentrations) of substances (volume fraction = st. m^3) of the substance per cubic meter of the bed)
P_S^c	capillary partial pressure of sulfur vapours
P_i^{in}	inlet concentration of ith substance
R	rate of sulfur condensation (s^{-1})
R_0	universal gas constant (kJ mol^{-1} K^{-1})
T	gas temperature (K)
T_{in}	inlet gas temperature (K)
T_{out}	gas temperature at the outlet from heat-exchanger (K)
T_W	the temperature of the heat-exchanger wall (K)
ΔT_{ad}	adiabatic heat rise (K) for reaction (superscript R) and condensation/evaporation (superscript P)
U	gas flow velocity, calculated for the full bed sequence and standard conditions (m s^{-1})
V	liquid sulfur molar volume (m^3 mol^{-1})
W	the rate of Claus reaction (s^{-1})
W_0	intrinsic rate of Claus reaction (s^{-1})
W_f	gas flow rate (st. m^3 s^{-1})
W_{surf}	reaction rate at the pellet surface
X	average liquid sulfur content of the catalyst bed
x	liquid sulfur content (degree of filling of catalyst pellet with liquid sulfur)
x_{init}	initial value of liquid sulfur content
Y	conversion
Y^*	equilibrium conversion

Greek letters

α	heat transfer coefficient in the catalyst bed (kJ m^{-3} K^{-1} s^{-1})
α_{he}	heat transfer coefficient in the heat-exchanger (kJ m^{-2} K^{-1} s^{-1})
β	mass transfer coefficient in the catalyst bed (s^{-1})
χ	propagation coefficient
ε	void fraction (porosity) of the catalyst bed
ε_p	void fraction (porosity) of the catalyst pellet
γ	heat capacity of the catalyst bed (kJ m^{-3} K^{-1})
η	effectiveness factor
φ, φ'	modified Thiele modulus
φ_0	basic Thiele modulus
λ_{eff}	effective coefficient of the catalyst bed frame heat conductivity (kJ m^{-2} K^{-1} s^{-1})
ν_i	stoichiometric coefficient for ith component in Claus reaction
θ	catalyst temperature (K)

θ_{init}	initial catalyst temperature (K)
$\prod$	concentrations product
ρ_S	density of liquid (with superscript L) and gaseous (superscript G) sulfur (kg st. m^{-3})
σ	coefficient of liquid sulfur surface tension
τ	time (s)
τ_c	cycle duration—time between flow reversals (s)
ω	velocity of condensation/evaporation front propagation ($m\,s^{-1}$)
ψ	boundary wetting angle

processes may be mentioned as commercially successful.

1. Processes based on Claus reaction performance at temperatures below the sulfur dew point (processes CBA, [6] and other works). Such method provides high equilibrium conversions in one catalyst bed, but it is complicated by requirement of periodic catalyst regeneration by sulfur evaporation at elevated temperatures. So such processes are usually performed in two or three (or even more) parallel reactors, periodically undergoing reaction and regeneration [6,8–12].
2. Processes based on selective oxidation of H_2S [13–15] by oxygen (Selectox, Superclaus, Oxysulfreen, etc.) using selective catalysts.
3. Processes applying absorption of unreacted H_2S with its following desorption and recycling back to Claus furnace (SCOT process [6]).

Though tail gas cleanup processes provide high recovery degree, the major part of sulfur is nevertheless produced in Claus furnace and main Claus catalytic stage. Looking at the history of process development one may state that during the more than 1960s years experience the basic technological principles of the main catalytic stage of the Claus process remained unchanged. All significant improvements have been made only in relation to the "head" of the process (Claus furnace) or to its "tail" (tail-gases cleanup units), not touching the "body"—main catalytic stage. The progress here was practically limited by development of new catalysts only.

The Boreskov Institute of Catalysis recently made some breakthrough in this area [16–19]. The essence of novel processes is application of reverse-flow technique [20] to the performance of Claus reaction, making possible the continuous process operation with inlet reaction mixture temperature below the sulfur dew point.

The flow-sheet of the single Claus reverse-process is shown at Fig. 1b. In this case the reaction mixture is fed to

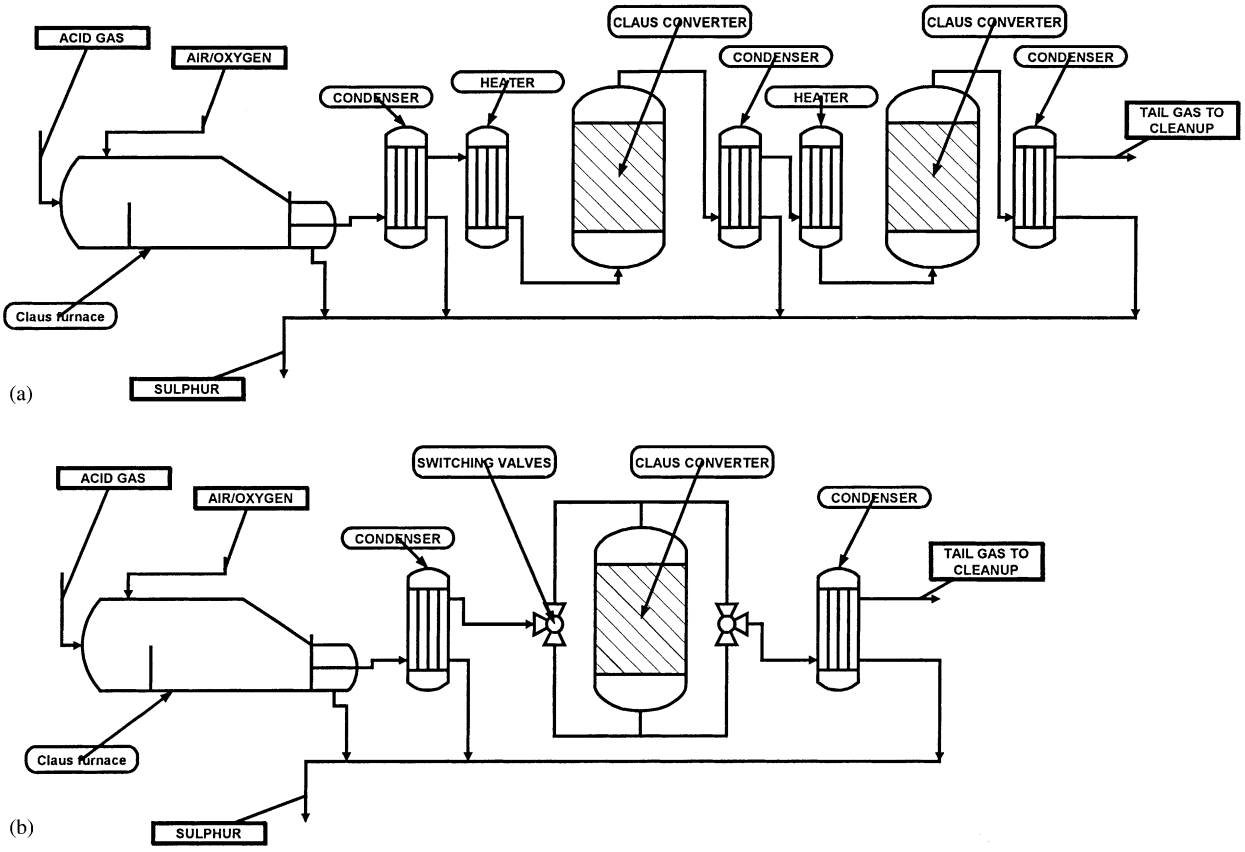

Fig. 1. Flow-sheets of the Claus process. (a) Conventional scheme, (b) reverse-process.

the catalytic reactor directly from the first condenser, without pre-heating. Reactor is operated under periodical gas flow reversals, which are provided by a system of switching valves.

Obviously, such process includes the complicated interaction of various phenomena (reaction, sulfur phase transitions, catalyst deactivation, etc.) and therefore the process development procedure must include detailed simulation before any pilot trials. This paper is dedicated to the mathematical modelling of Claus reactors and Claus process flow-sheets with account of sulfur condensation and evaporation in catalyst bed both in conventional and reverse-flow regimes.

2. Mathematical model of the process

Quite a few investigations have been made earlier in the area of simulation of the Claus process in the packed catalyst bed under the conditions of sulfur condensation. The most interesting is the work [21], where authors describe the temperature and sulfur condensation fronts, moving in the catalyst bed with maximum temperature gradually decreasing with time. Authors of the present paper, earlier published parts of their results [18,19,22,23] related to the modelling of the Claus reverse-process.

2.1. Construction of the model

The whole and complete mathematical model of such complicated non-stationary process, accounting for non-linear kinetics and phase transfer and interaction between them is extremely complex and cannot be used for simulation purposes. Thus, it became necessary to construct the simplified model, which will provide both the fast calculations and the adequate qualitative and quantitative description of the simulated system. The well-known approach based on division of all phenomena into separate levels according to characteristic time and space scales [24,25], was used as the general basis for model creation. The unsteady-state model for the packed bed in that case usually contains five levels: (1) catalyst surface (reaction kinetics), (2) catalyst pellet (heat and mass transfer inside the pellet), (3) catalyst bed element (heat and mass transfer between reaction mixture and the pellet), (4) catalyst bed (reactor), and (5) process flow-sheet (catalyst beds, heat-exchangers, etc.).

The further conventional assumptions were used to construct the model.

1. The gas flow velocity, concentration and temperature distribution along the bed radius is uniform. The bed is adiabatic.
2. Outer surface of the catalyst pellet has equal access for the reaction mixture in all points.
3. The processes of mass transfer inside the pellets are quasi-steady-state in relation to heat transfer processes in the catalyst bed.
4. Temperature gradients inside the catalyst pellet are absent. This assumption is confirmed by the results of [26], showing isothermicity of the catalyst pellet in the Claus reaction and by our own estimations.
5. The aggregate of all chemical reactions, occurring on the catalyst surface may be described by one general equation:

$$H_2S + \frac{1}{2}SO_2 \Rightarrow \frac{1.5}{n}S_n + H_2O \tag{3}$$

where n is number of sulfur atoms in averaged sulfur molecule. Actually sulfur vapours may contain all sulfur molecules from S_2 to S_8, which may transfer into each other and with distribution between them changing with temperature. Assuming the very fast transfer rate it is possible to use the n value corresponding to average equilibrium in typical process conditions. For temperature range 120–300 °C, the reasonable value is $n = 6$. The similar approach was applied in [21,26,27].

6. Decrease of Claus reaction rate due to the blockade of active surface by condensed sulfur linearly depends upon the degree of the catalyst filling by liquid sulfur

$$W = W_0(1 - x) \tag{4}$$

That dependence was experimentally proved in [28].

7. Formed sulfur condenses only inside the catalyst pellet. The rate of achievement of equilibrium between sulfur vapours concentration near the catalyst surface and equilibrium value for saturated vapours during condensation and evaporation is assumed to be infinitely high. In other words, the existence of overheated liquid or overcooled vapour is reasonably ignored.
8. The changing of the reaction mixture volume in the course of the reaction is negligibly small due to relatively low reagent concentrations and not high difference in number of moles between reagents and products.
9. Heat capacity of the catalyst filled with liquid sulfur linearly depends upon the content of liquid sulfur

$$\gamma = C_c + (1 - \varepsilon)\varepsilon_p x C_S^L \tag{5}$$

Given assumptions make possible to construct the three-phase one-dimensional model, accounting for interaction between H_2S and SO_2 with possible condensation and evaporation of formed sulfur, reversible catalyst deactivation by liquid sulfur, heat and mass transfer between pellets and reaction mixture, catalyst frame heat conductivity, etc.

The mass balance equations for all substances except sulfur may be written as follows:

$$\beta_i(P_i - \hat{P}_i) + \nu_i W = 0 \tag{6}$$

$$U\frac{\partial P_i}{\partial \ell} + \beta_i(P_i - \hat{P}_i) = 0 \tag{7}$$

The following mass balance equations may be used for sulfur:

$$\beta_S(P_S - \hat{P}_S) + \nu_S W - aR = 0 \tag{8}$$

$$U\frac{\partial P_S}{\partial \ell} - \nu_S W + aR = 0 \quad (9)$$

$$R = \frac{dx}{d\tau} \quad (10)$$

$$a = \frac{(1-\varepsilon)\varepsilon_p \rho_S^L}{\rho_S^G} \quad (11)$$

The conditions of sulfur vapour–liquid phase transfer are the following condensation occurs when $\hat{P}_S > P_S^*$ (if $x < 1$) and evaporation $\hat{P}_S < P_S^*$ and $x > 0$. If such conditions are satisfied then Eqs. (8)–(11) are used with the consequence of Assumption 6

$$\hat{P}_S > P_S^* \quad (12)$$

In the opposite case Eqs. (6) and (7) are applied.

The heat-exchange between the gas mixture and the catalyst is described by equation

$$U\frac{\partial T}{\partial \ell} + \alpha C_p(T-\theta) = 0 \quad (13)$$

The heat balance for the catalyst bed element may be formulated in a general form

$$\frac{\partial(\gamma\theta)}{\partial\tau} = \lambda_{eff}\frac{\partial^2\theta}{\partial\ell^2} - U\frac{\partial H_G}{\partial\ell} \quad (14)$$

With account of Eqs. (5) and (10) the left part of Eq. (14) may be transformed into

$$\frac{\partial(\gamma\theta)}{\partial\tau} = \gamma\frac{\partial\theta}{\partial\tau} + \theta(1-\varepsilon)\varepsilon_p C_S^L R \quad (15)$$

The second term of the right part in Eq. (14) may be transferred to

$$U\frac{\partial H_G}{\partial\ell} = U\frac{\partial\sum H_i}{\partial\ell} = U\frac{\partial\sum(C_i P_i T)}{\partial\ell} \quad (16)$$

$$U\frac{\partial\sum(C_i P_i T)}{\partial\ell} = U\sum(C_i P_i)\frac{\partial T}{\partial\ell} + UT\frac{\partial\sum(C_i P_i)}{\partial\ell} \quad (17)$$

Assuming $\sum(C_i P_i) = C_p$ and applying Eq. (13) the first term of the right part in Eq. (17) is transformed as follows:

$$U\sum(C_i P_i)\frac{\partial T}{\partial\ell} = \alpha(\theta - T) \quad (18)$$

The second term of Eq. (13) may be differentiated under assumption of constancy of components heat capacities

$$UT\frac{\partial\sum(C_i P_i)}{\partial\ell} = \sum\left(C_i UT\frac{\partial P_i}{\partial\ell}\right) \quad (19)$$

$$\sum\left(C_i UT\frac{\partial P_i}{\partial\ell}\right) = TW\sum(\nu_i C_i) - aRTC_S^G \quad (20)$$

Taking into account, transformations (15–20) and that $T\sum(\nu_i C_i) = -QR$, the heat balance equation may be formulated as follows:

$$\gamma\frac{\partial\theta}{\partial\tau} = \lambda_{eff}\frac{\partial^2\theta}{\partial\ell^2} + \alpha(T-\theta) + Q_p W + (1-\varepsilon)\varepsilon_p R\left(T\frac{C_S^G\rho_S^L}{\rho_S^G} - \theta C_S^L\right) \quad (21)$$

what may be simplified by account of $T(C_S^G\rho_S^L/\rho_S^G) = TC_S^L + Q_p$

$$T\frac{C_S^G\rho_S^L}{\rho_S^G} - \theta C_S^L = Q_p + C_S^L(T-\theta) \quad (22)$$

Q_p value is significantly higher than numerical value of C_S^L, so the last term of Eq. (22) may be neglected, because it may visibly act only under significant difference between gas and solid phase, what is not typical for such processes. Thus, the heat balance equation for the solid phase may be given in a final formulation

$$\gamma\frac{\partial\theta}{\partial\tau} = \lambda_{eff}\frac{\partial^2\theta}{\partial\ell^2} + \alpha(T-\theta) + Q_p W + (1-\varepsilon)\varepsilon_p R Q_p \quad (23)$$

The model should be accomplished by the boundary conditions

$$\ell = 0 \Rightarrow \begin{cases} T = T_{in} \\ \lambda_{eff}\dfrac{\partial\theta}{\partial\ell} = 0 \\ P_i = P_i^{in} \end{cases} \quad (24)$$

$$\ell = L \Rightarrow \lambda_{eff}\frac{\partial\theta}{\partial\ell} = 0 \quad (25)$$

$$\tau = 0 \Rightarrow \begin{cases} \theta(\ell) = \theta_{init} \\ x(\ell) = x_{init} \end{cases} \quad (26)$$

2.2. Reaction kinetics

A lot of attention has been earlier paid to experimental investigations of the Claus reaction kinetics [29–31] on various catalysts. The most representative form of the rate equation for the Claus reaction on γ-Al_2O_3, accounting for the reversibility of the reaction was published in [21,29]

$$W = K_1\frac{\hat{P}_{H_2S}\hat{P}_{SO_2}^{0.5} - \hat{P}_{H_2O}\hat{P}_{S_6}^{0.25}/K_p}{(1+K_2\hat{P}_{H_2O})^2} \quad (27)$$

where

$$K_1 = K_0\exp\left(-\frac{E_a}{R_0\theta}\right) \quad (28)$$

This equation and kinetic parameters given by authors of [29] were used for mathematical modelling of the process. It should be noted that Eq. (27) gives the reaction rate without account of intraparticle diffusion limitations and influence of sulfur condensation and evaporation. These questions should be discussed separately.

2.3. Influence of intraparticle diffusion limitations

Application of the full private derivatives mathematical model of the catalyst pellet [32] for calculation of observed reaction rate leads to the sufficient complication of the catalyst bed model, especially for the unsteady-state case with its typical time-consuming calculations. To simplify the model it was proposed to use estimation technique, based on application of Thiele modulus. In general the application of Thiele modulus is accurate only for the first order irreversible reaction in the isothermal catalyst pellet. The original approach was described in [26], where authors confirmed the isothermicity of the pellet, using McGreavy–Cresswel criterion [33], and proposed the modified Thiele modulus, adequately describing the variation of the efficiency factor:

$$\varphi' = \frac{\varphi_0}{\sqrt{1 - P^*_{H_2S}/P_{H_2S}}} \tag{29}$$

Unfortunately, the proposed modification is not very convenient in direct use (because it requires the value of the equilibrium H_2S concentration, which may be calculated only by iterative procedure) and authors [26] have not proposed the final equation, connecting Thiele modulus with efficiency factor.

To solve these problems the following approach was proposed. Let us consider the product of substances concentrations:

$$\prod = \prod_i (P_i^{\nu_i}) = \frac{P_{S_6}^{0.25} P_{H_2O}}{P_{H_2S} P_{SO_6}^{0.5}} \tag{30}$$

In the equilibrium state, $\prod = K_p$. If we will divide $\prod$ for some arbitrary composition by equilibrium constant at given temperature K_p, then we will obtain

$$\frac{\prod}{K_p} = \frac{P_{S_6}^{0.25} P_{H_2O}}{(P^*_{S_6})^{0.25} P_{H_2O}} \frac{P^*_{H_2S} (P^*_{SO_2})^{0.25}}{P_{H_2S} P_{SO_2}^{0.5}} \tag{31}$$

Sulfur has low stoichiometric coefficient and is represented in $\prod$ with small power (0.25) so Eq. (31) may be simplified into (if sulfur concentration on the outer surface is not equal to zero)

$$\frac{P_{S_6}^{0.25}}{(P^*_{S_6})^{0.25}} \approx 1 \tag{32}$$

Furthermore, in typical reaction conditions the water vapours content is usually high (20% and more), so the relative change of water concentration due to the reaction is not high and the following may be accepted:

$$\frac{P_{H_2O}}{P^*_{H_2O}} \approx 1 \tag{33}$$

Claus process is usually performed with H_2S/SO_2 concentrations ratio closed to stoichiometric

$$P_{H_2S} \approx 2 P_{SO_2} \tag{34}$$

With account of Eqs. (32)–(34), Eq. (31) is transformed into

$$\frac{\prod}{K_p} \approx \left(\frac{P^*_{H_2S}}{P_{H_2S}} \right)^{1.5} \tag{35}$$

and thus Eq. (29) may be rewritten as:

$$\varphi' = \frac{\varphi_0}{\sqrt{1 - (\prod / K_p)^{2/3}}} \tag{36}$$

Π may be easily determined from the gas composition on the outer catalyst pellet surface according to (30). To account the difference of the Claus reaction from the first order one, let us consider the equation for such transformation, proposed in [32]:

$$\varphi' = \varphi \sqrt{\frac{m+1}{2}} \tag{37}$$

Applying assumption (34) the value of 1.5 may be proposed for the rate order of Claus reaction versus SO_2 concentration:

$$W \sim K_1 P_{H_2S} P_{SO_2}^{0.5} \sim 2 K_1 P_{SO_2}^{0.5} \tag{38}$$

So, Eq. (37) transforms into

$$\varphi = \varphi' \sqrt{1.25} \tag{39}$$

Resulting equation for modified Thiele modulus may be expressed as

$$\varphi = \frac{d}{2} \sqrt{\frac{1.25 W_{surf}}{P^{surf}_{SO_2} D^{eff}_{SO_2} (1 - (\prod / K_p)^{2/3})}} \tag{40}$$

Thus, the efficiency factor for the reaction may be calculated via conventional equation [32] for the sphere-shaped pellet

$$\eta = \frac{3}{\varphi} \left(c\mathrm{th}\, \varphi - \frac{1}{\varphi} \right) \tag{41}$$

using the proposed modification of the Thiele modulus (40).

Of course, the proposed method is not strict due to a lot of assumptions and simplifications. It is necessary to prove the accuracy of efficiency factor calculations. To test the accuracy the following procedure was performed. The conditions of the reaction performance (reaction mixture composition, temperature and pellet size) were generated by random variation in reasonable range. Then two computations were made for each case: solution of the full mathematical model of the catalyst pellet with calculation of the observed reaction rate and simplified calculations of modified Thiele modulus via Eqs. (40) and (41).

Fig. 2 demonstrates the obtained results. Here the solid line corresponds to the function (41). The efficiency factor, obtained from solution of the full model, was plotted versus Thiele modulus value, obtained from (40). It is seen that in general the proposed method provides adequate estimations of efficiency factor in a wide range of reaction conditions. The average deviation was equal to ~4% (with maximum deviation of ~10%), what does not exceed the typical accuracy of rate measurements in kinetic experiments. Thus,

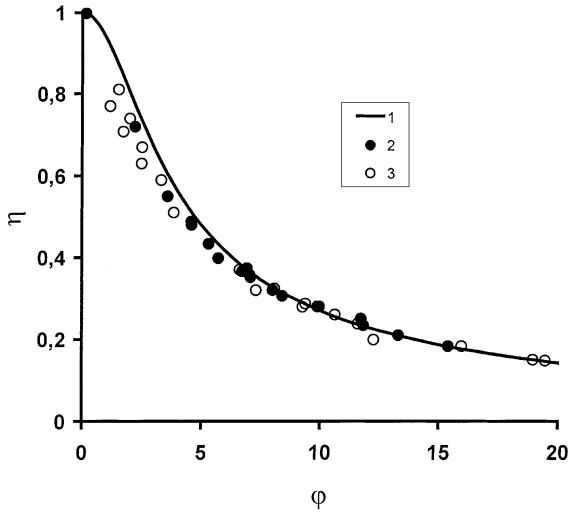

Fig. 2. Effectiveness factor η plot vs. modified Thiele modulus φ. Curve (1), function (41); curve (2) full solution for stoichiometric mixtures; curve (3) full solution for non-stoichiometric mixtures.

it was statistically confirmed that the proposed simplified method might be applied in the packed bed modelling.

The special calculations for non-stoichiometric mixtures showed that such method may be also applied, but with addition of empirical term, accounting for variation of H_2S/SO_2 ratio. That modification allows obtaining solutions for such cases with average deviation from accurate solution not exceeding ~7%, what also satisfies the requirements for process calculations (see also Fig. 2).

2.4. Efficiency factor in conditions of sulfur condensation

This part of the investigation was published earlier in details in [34]. Here we will only reproduce some basic conclusions.

Sulfur condensation inside the catalyst pellet may occur in three different regimes.

1. When the pellet temperature is equal to the sulfur vapours dew point temperature, the condensation of formed sulfur may occur inside the pellet due to intraparticle diffusion resistance in the course of reaction. It was shown that in that case the reaction rate decreases linearly with the rise of liquid sulfur content in the pellet.
2. When the pellet temperature is higher than the dew point, then no condensation at all may occur or condensation may arise only in the centre of the pellet due to intraparticle diffusion resistance. In that case the sulfur content does not have any visible effect on reaction the rate.
3. When the pellet temperature is below the dew point the condensation occurs in the outer part of the pellet (pore mouth). In that case reaction rate falls dramatically and becomes 0 at $x < 1$, but probability of such regime in the process conditions is not high.

Summarising these results it may be stated, that Eq. (4) is valid not only for the catalyst surface level, but for catalyst pellet as well. Thus, the observed rate of the reaction may be described by the following equation:

$$W = W_0\eta(1 - x) \tag{42}$$

2.5. Influence of capillary pressure

The questions of influence of capillary pressure in catalyst pores on sulfur condensation and evaporation have been discussed in [27]. It was shown that during condensation the sulfur deposition occurs in radial direction (from pore walls to pore axis), while evaporation occurs in axial direction (from pore end to pore mouth), thus giving the condensation–evaporation hysteresis. The influence of capillary pressure may be estimated from equations

$$d_p = -\frac{2\sigma V}{R_0\theta \ln(P_S^c/P_S^*)} \quad \text{(for condensation)} \tag{43}$$

$$d_p = -\frac{4\sigma V \cos\psi}{R_0\theta \ln(P_S^c/P_S^*)} \quad \text{(for evaporation)} \tag{44}$$

2.6. Determination of other model parameters

The part of model parameters may be defined from the reference literature: $C_c = 1228\,\mathrm{kJ\,m^{-3}\,K^{-1}}$, $C_p = 1.307\,\mathrm{kJ\,st.\,m^{-3}\,K^{-1}}$, $C_S^L = 2095\,\mathrm{kJ\,m^{-3}\,K^{-1}}$, $Q_p = 1.28 \times 10^5\,\mathrm{kJ\,st.\,m^{-3}}$. Stoichiometric coefficients are determined from reaction Eq. (3).

Transfer coefficients and coefficient of heat conductivity of the catalyst bed frame were calculated from empirical criteria equations [35]. Test calculations showed that there is no need to account for the dependence of transfer coefficients from current temperatures—it is enough to calculate them once for some basic temperature for typical process conditions (e.g. 250 °C). Such approach provides the sufficient rise of calculation speed, not visibly decreasing its accuracy.

The void fraction of the bed ε of spheres or cylindrical pellets may be taken equal to 0.4 [35]. The porosity of the Claus catalyst pellets p varies in the range of 0.15–0.65 [36] and the typical value for γ-Al_2O_3 may be taken equal to 0.5.

Equilibrium concentration of sulfur in saturated vapours (for S_6) is given as a function from temperature [27]

$$\ln P_{S_6}^*(T) = 3.9628 - \frac{2500.12}{T - 86.85} \tag{45}$$

Our own thermodynamic investigations gave the expression for dependence of Claus reaction equilibrium constant from temperature

$$\ln K_p(T) = \frac{5910}{T} + 1.13 \times 10^{-3}T - 1.038 \ln T \tag{46}$$

Thermodynamic studies also gave the heat of reaction $Q = 2330\,\mathrm{kJ/m^3}$ of converted H_2S (at standard conditions). The

density of liquid and gaseous sulfur were calculated via equations [27]

$$\rho_S^L = 2036.3 - 0.60137T \quad (47)$$

$$\rho_S^G = \frac{2926.4}{T} \quad (48)$$

Effective diffusion coefficient $D_{SO_2}^{eff}$ for Eq. (40) was calculated using equation

$$D_{SO_2}^{eff} = \chi \left(\frac{1}{(1/D_{mol}) + (1/D_{kn})} \right) \quad (49)$$

where propagation coefficient χ was taken equal to 0.2 according to our own experimental data. Knudsen diffusion coefficient D_{kn} was calculated for the catalyst with uniform pore size distribution though the model may also be applied as well for the catalyst with other type of pore size distribution.

2.7. Numerical method of model solution

Obviously the proposed model (4–49) does not have the analytical solution. The numerical method, based on indirect balance difference approximations [37], was developed to solve the problem.

The application of balance difference approximations provides the obtaining of non-negative numerical solutions. The method applied the space grid, uniform along the length of the catalyst bed. The iterative process for each time step consisted of two levels: at the first one (inner level) equations of the mass balance (6–12) were solved together with kinetic Eqs. (27) and (42) (with calculation of effectiveness factor via Eqs. (40) and (41)) at every space point, and at the second, external, level the heat balance Eqs. (13) and (23) were solved by run-through method [37]. The time step varied from 0.1 to 10 s, depending upon the number of iterations at the second level.

The software created on the base of described algorithm gave way to perform calculations of the reactors with periodical reversals of the gas flow. The structure of the software allows to construct the computer programs for simulation of various process flow-sheets, including multi-reactor schemes with heat-exchangers (heaters and condensers), bypass lines and mixing junctures, etc.

3. Mathematical modelling of the process

All calculations were performed for the following process conditions:

- inlet gas composition: H_2S, 5% (vol.%); SO_2, 2.5%; H_2O, 20%; S_6, 0.5%; and remaining nitrogen;
- inlet gas temperature, −140 °C;
- initial bed temperature, −250 °C;
- linear gas velocity in the catalyst bed, 0.5 m/s;
- the catalyst, γ-Al_2O_3; pellets, spheres, 5 mm diameter; average pore radius, 200 Å;
- gas residence time in the bed, 5 s.

This set of parameters was taken as the basis for computation. Given values were also varied in the calculations (that will be specified in the text).

3.1. Sulfur condensation and evaporation fronts

The purpose of this study was to simulate the propagation of sulfur condensation and evaporation fronts. The condensation may occur when the reactor is fed by the reaction gas with low temperature (below the dew point). Such regime is called ‘Cold Bed Adsorption’ and it is widely applied in industrial processes of sulfur recovery [6,8–12] to obtain high conversion at low temperature, which is thermodynamically favourable.

According to simulation results, in the beginning of the process the propagation of the heat wave is observed in the bed. Such wave is connected with the cooling of the pre-heated bed to the temperature, corresponding to the inlet gas one. It is interesting to note that the similar wave is observed also in the case with lower initial catalyst bed temperature, then this wave is connected with bed heating. The velocity of propagation of such waves is in good agreement with estimation of heat front velocities [24,25]. At the end of this transient period the quasi steady-state temperature and concentration profiles are formed. The outlet gas temperature in this state exceeds the inlet one by the value of adiabatic heat rise, corresponding to equilibrium conversion.

Fig. 3 demonstrates the evolution of temperature and concentrations fields in time under feeding of low temperature gas into the pre-heated catalyst bed. The first curve shows the temperature and concentration distribution after the completion of aforementioned transient period. The catalyst temperature in the inlet part of the bed is below the formed sulfur dew point, so sulfur is condensed here. Sulfur condensation leads to the deactivation of the catalyst in this zone thus shifting the reaction zone in the direction of the gas flow filtration. Such shift gives rise to the propagation of the slow heat and concentration fronts, which may be called the condensation front. Such front is characterised with constant temperature and concentration gradients along the bed length.

It is interesting to compare these results with the data of [21], where the sulfur condensation front has the similar gradients, decreasing with time. Authors of [21] assumed the rate of sulfur deposition equal to the rate of its formation, not taking into account its possible transfer along the bed with reaction mixture. Such groundless simplification caused the qualitative difference in solutions. At the same time, our results are confirmed by investigation [38], where the propagation of fronts, connected with adsorption of the reaction mixture component causing the non-selective catalyst deactivation, is observed.

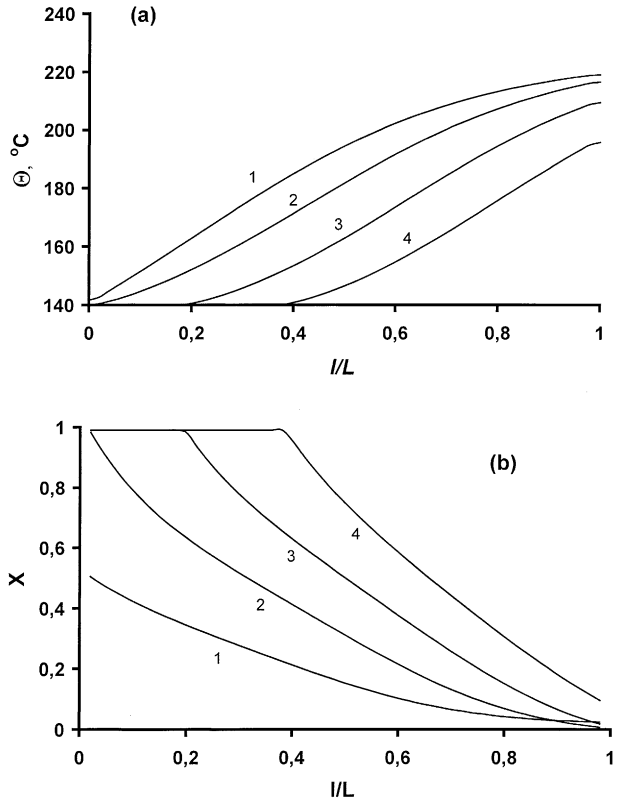

Fig. 3. Propagation of sulfur condensation front: catalyst temperature (a), and liquid sulfur content (b) profiles along the bed length. Numbers on the curves corresponds to the time from the process start-up (in 1000 s).

The characteristic time of filling the pellet by sulfur is significantly higher than characteristic time, connected with catalyst heat capacity inertia, so the propagation velocity of the heat front is much less than for conventional heat front and may be estimated from mass balance equations. Assuming the achievement of the equilibrium conversion, corresponding to the outlet temperature, and taking into account that outlet temperature exceeds the inlet one by the value of adiabatic heat rise, the velocity of condensation front may be expressed in a following way:

$$\omega = \frac{U\rho_S^G}{\rho_S^G(1-\varepsilon)\varepsilon_p}(\nu_S P_{H_2S}^{in} Y^* P_{S_6}^{in} - P_S^*(\theta_{max})) \quad (50)$$

where outlet temperature is defined by

$$\theta_{max} = T_{in} + \Delta T_{ad}^R Y^* + \Delta T_{ad}^P \quad (51)$$

Eqs. (50) and (51) may be also used for estimation of the parameters of evaporation front, which may exist under feeding of high temperature gas into the bed of catalyst, filled by liquid sulfur. In both cases, Eqs. (50) and (51) provide good coincidence with the results of full numerical simulation. It is necessary to note, that Eqs. (50) and (51) remain strongly valid for long catalyst beds (with the length higher than the width of the reaction zone), though the velocity of the temperature marking shifting may be estimated from these equations in the shorter beds as well.

Parametric studies showed that condensation front velocity rises with increase of gas flow filtration and sulfur concentration in the inlet gas and with decrease of inlet gas temperature. The reagents concentration influence is more complex and shows the maximum of velocity. From one hand, in the area of low concentrations the front velocity rises with increase of concentration due to the rise of total sulfur amount in the inlet gases. On the other hand, further concentration rise leads to the increase of maximum (adiabatic) bed temperature, thus providing the decrease of the front velocity. For given conditions, the maximum velocity is obtained at H_2S concentration of ~5%.

The obtained qualitative and quantitative results are in good agreement with the industrial data of operation of processes, applying the 'Cold Bed Adsorption' regime.

3.2. Simulation of the reverse-flow reactor

Let us consider, the packed catalyst bed undergoing the periodical flow reversals, when the inlet gas temperature is below the sulfur dew point one [16–19,22,23]. As it was shown above in that case the condensation front starts to propagate in the inlet part of the bed. Obviously, if such front will reach the end of the bed, the process will fade and the regeneration of the catalyst will be necessary.

If we will change the direction of gas flow filtration to the opposite one after some time after the start of the procedure (e.g. 1000 s), then the similar front will start moving from the opposite end of the bed. At the same time, the part of previously condensed sulfur will be evaporated by the heat of the reaction. Nevertheless, during the few first reversal cycles the total sulfur contents of the bed will rise, though the rate of its rising will decrease from cycle to cycle. Deactivation of the catalyst in the bed ends will intensify the regenerative heat-exchange here, leading to the gradual rise of the catalyst in the central part of the bed.

After few cycles the rates of sulfur condensation and evaporation will become equal and the total content of the liquid sulfur in the bed, averaged per cycle duration, will become constant. The typical temperature and sulfur content profiles in such stabilised unsteady-state regime within the cycle are given in the Fig. 4a and b. It is seen, that given profiles in the beginning and in the end of the cycle are symmetrical versus the bed centre. The stabilised character of the process is also confirmed by satisfaction of total mass and heat balances requirements. Thus, the process has the repeating nature and may be operated during unlimited time in continuous mode, without stops for catalyst regeneration from liquid sulfur, despite the low inlet gas temperature.

In other words, the process provides evaporation of liquid sulfur by means of reaction heat emission. The catalyst bed is separated into three parts: two bed ends are practically deactivated by sulfur and play the role of regenerative heat-exchangers, while the central part remain active,

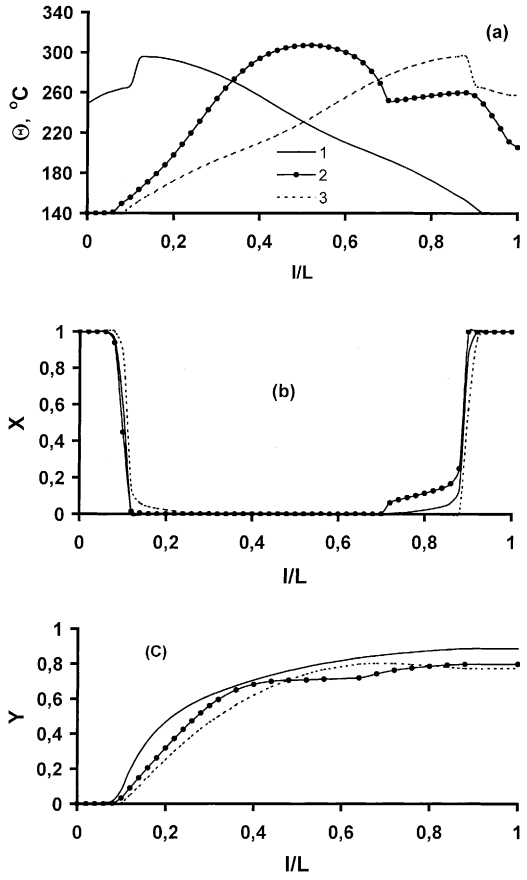

Fig. 4. Established unsteady-state regime under periodical flow reversals: profiles of catalyst temperature (a), liquid sulfur content (b), and conversion (c) vs. bed length. Curves 1–3, the beginning, middle and end of the cycle, respectively. Cycle duration $\tau_c = 2000$ s.

providing reaction occurrence. Condensation and evaporation of sulfur within the cycle occurs mainly in the narrow borders between these areas.

Fig. 4c shows the H_2S conversion profiles along the bed during the cycle. In general, the reverse-process provides higher conversion, than the steady-state one. It may be expressed by the following. The limit conversion in the conventional process is generally defined by equilibrium conditions, in particular, by outlet temperature. The outlet temperature, here, is equal to the inlet one plus adiabatic heat rise, while the minimum inlet temperature is limited by the sulfur dew point. For the given gas composition, the dew point temperature is equal to ∼230 °C and the corresponding outlet temperature in the adiabatic reactor will reach ∼290 °C with corresponding equilibrium conversion of ∼73%. The reverse-process makes possible to perform the process with maximum temperature, only slightly exceeding the dew point (e.g. 250 °C), thus providing higher equilibrium conversion (∼92%). It is seen from the Fig. 4c, that decreased temperature at the outlet bed end in the beginning of the cycle provides also an additional gain in conversion due to the favourable thermodynamic conditions.

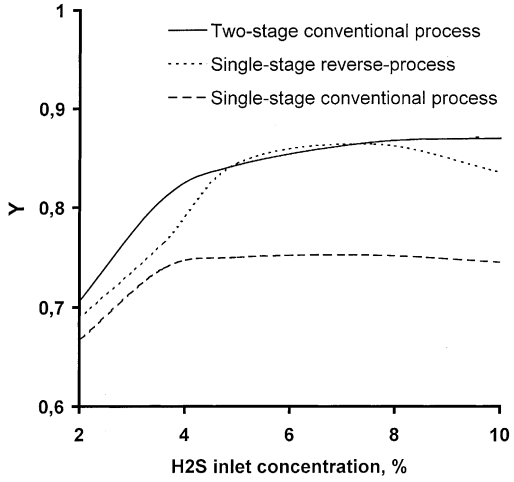

Fig. 5. Hydrogen sulphide conversion vs. inlet concentration of H_2S (in vol.%). Sulfur recovery in Claus furnace is not taken into account.

Fig. 5 demonstrates the dependence of the calculated H_2S maximum conversion upon the hydrogen sulphide concentration in the inlet gas for conventional processes and the reverse-process. It is evident, that the reverse-process provides higher conversions, than conventional reactor, in all concentration area. Moreover, in the area of medium concentrations (quite typical for the majority of the industrial Claus plants) that reverse-flow reactor appears to be more efficient, than a two-stage steady-state process, comprising two reactors with intermediate sulfur condensation.

Let us consider, in more details the influence of various process parameters on process characteristics.

3.2.1. The cycle duration τ_c

The Fig. 4 demonstrates the typical profiles for the medium cycle duration. The corresponding profiles for the shorter cycles (500 s) are given in Fig. 6. Here, the different

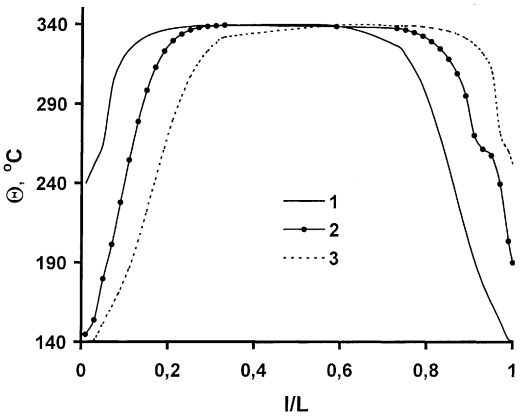

Fig. 6. Catalyst temperature profiles vs. bed length in the established unsteady-state regime with short cycles. Curves, 1–3, the beginning, middle and end of the cycle, respectively. Cycle duration $\tau_c = 500$ s. $T_{in} = 140$ °C.

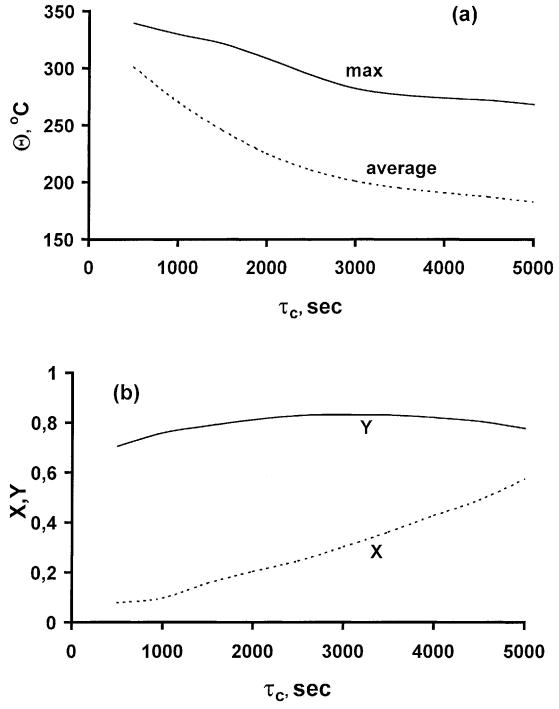

Fig. 7. Dependence of Claus reverse-process parameters upon the cycle duration: catalyst temperature (a), liquid sulfur content and conversion (b). max: maximum catalyst temperature in the cycle, average catalyst temperature, averaged per bed length and cycle duration.

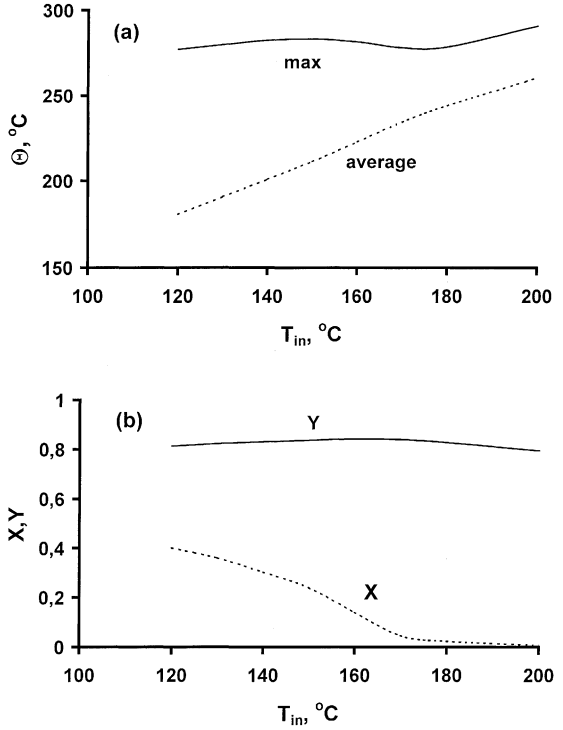

Fig. 8. Dependence of Claus reverse-process parameters upon the inlet gas temperature: catalyst temperature (a), liquid sulfur content, and conversion (b).

picture is observed: no visible migration of heat and concentrations waves is seen. The temperature profile consists of high temperature plateau in the central part of the bed and oscillating low temperature 'wings' at the end parts from both sides. The liquid sulfur content of the bed in that case is minimum.

On the contrary, the longer cycles are characterised by more expressed movement of heat and concentration profiles, getting closer to the simple propagation of condensation fronts, described above. Obviously, increasing of the cycle duration over some critical value leads to the dramatic rise of liquid sulfur content of the catalyst bed, followed by process fading due to the catalyst deactivation.

The influence of τ_c on process parameters is given in Fig. 7. It is seen, that the rise of τ_c leads to the increase of the liquid sulfur content and the decrease of maximum temperature of the bed. In the area of short cycles, the reaction zone, free from liquid sulfur, is wide enough to provide the achievement of reaction equilibrium, so here, the decrease of the maximum temperature with the rise of τ_c causes the increase of H_2S conversion. In longer cycles, the reaction zone is getting smaller due to the rise of sulfur content with τ_c, so the conversion becomes kinetically controlled. In that area the conversion decreases with the rise of τ_c. In general, it explains the existence of maximum conversion at some optimal cycle duration.

Inlet temperature T_{in} influence on process parameters is demonstrated in the Fig. 8. It is seen that maximum temperature practically does not depend upon the inlet one in area below 170 °C (for given conditions). After 170 °C, the maximum temperature starts to rise linearly with T_{in}. The critical temperature (here, −170 °C) is characterised by the qualitative change of the situation—at this temperature (and higher) all sulfur is evaporated from the outlet bed end, while at lower temperatures it only the partial evaporation occurs. Evidently, the real value of the critical temperature will depend upon many process parameters (inlet gas composition, cycle duration, etc.), but it is important because the maximum conversion is observed exactly in this area. For lower T_{in} the conversion decreases due to the rise of sulfur content, leading to the shortening of the reaction zone, while higher inlet temperature, leading to higher reaction temperatures, is less favourable from the reaction equilibrium point of view. It is necessary to note that temperature 140–170 °C is typical for the Claus condenser outlet, so the reaction gas in this process may be fed from the preliminary condenser into the reactor without pre-heating.

Linear gas velocity U influences the external heat and mass transfer parameters, what must be reflected in the simulation results. Nevertheless, the computations showed that the real influence (at constant gas residence time) is rather small. Probably, the internal transfer limitations are more pronounced, than the external one.

Inlet concentration of H_2S (with stoichiometric concentration of SO_2) influence on process parameters is given in Fig. 9. Decrease of H_2S content to 2% (vol.%) gives the

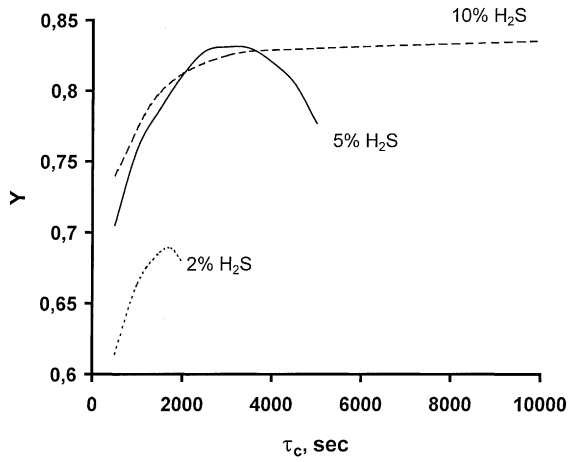

Fig. 9. Hydrogen sulphide conversion in the Claus reverse-process for different inlet concentrations of H_2S (in vol.%) vs. cycle duration. Sulfur recovery in Claus furnace is not taken into account.

decrease of the conversion due to worsening of equilibrium conditions, and the water and sulfur vapours concentration remain constant. More over the decrease of concentration leads to lower reaction heat emission and to lower maximum catalyst temperature, giving the rise of sulfur content. In this case, the optimal and maximum cycle duration are decreased as well. The rise of the H_2S concentration to 10% provide high reaction heat emission, causing the effective sulfur evaporation from the outlet bed end in each cycle, thus widening the reaction zone and increasing the conversion, as well as optimal and maximum cycle duration.

Catalyst pellet size influences significantly the parameters of heat and mass transfer both inside and outside the pellet. Fig. 10 shows dependence of process parameters upon the pellet diameter (for sphere-shaped pellets). It is evident that intensification of internal and external transfer processes with decrease of d leads to the rise of conversion. The application of small-sized pellet in the process is preferred, though actually the reasonable minimum size may be defined from pressure drop limitations.

3.2.2. Catalyst activity

Fig. 11 shows the influence of catalyst intrinsic activity (varied by variation of pre-exponential factor in the kinetic Eqs. (27) and (28)). The conversion rises with the rise of K_0. This fact is also evident for the steady-state process, but in the last one the maximum conversion will be limited by equilibrium. In the reverse-process the increase of catalyst activity also provide the decrease of maximum temperature, because the reaction will occur faster in the low temperature zone and the reaction mixture will enter the high temperature part of the bed more converted, decreasing the heat emission here. Thus, the increase of catalyst activity under reverse-flow operation can improve thermodynamic conditions, though the conversion will be also thermodynamically limited.

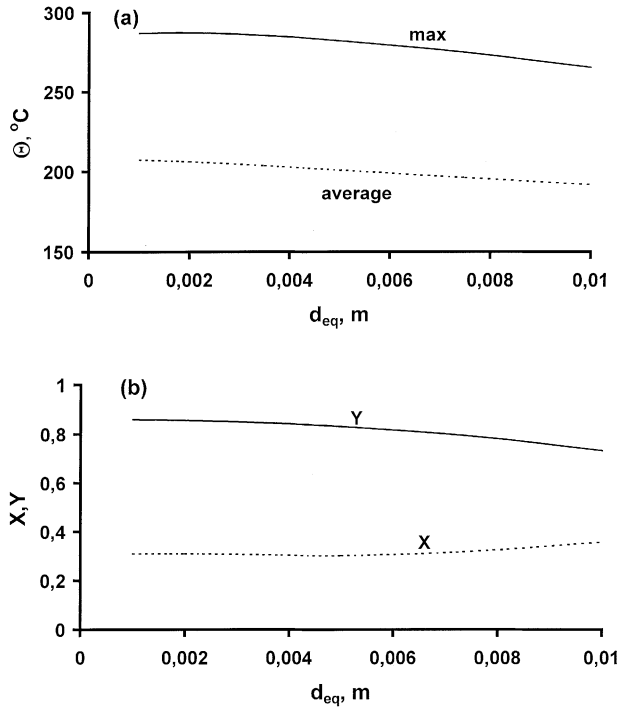

Fig. 10. Dependence of Claus reverse-process parameters upon the equivalent diameter of the catalyst pellet, catalyst temperature (a), liquid sulfur content and conversion (b).

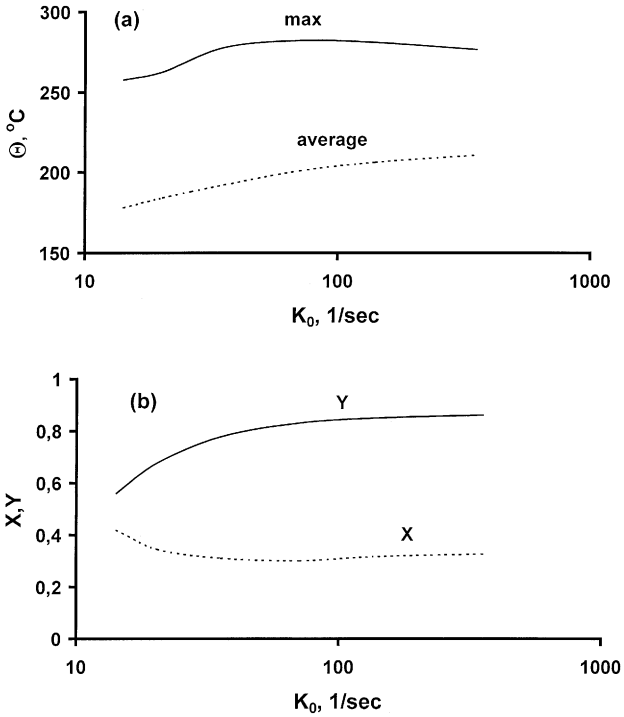

Fig. 11. Dependence of Claus reverse-process parameters upon the catalyst activity (given by the variation of pre-exponent K_0, basic value of K_0 is $70.1\,s^{-1}$): catalyst temperature (a), liquid sulfur content and conversion (b).

3.3. The two-stage reverse-process

The calculations showed that single-stage reverse-process provides higher conversion, than conventional steady-state one, though in some cases it may be not sufficient. To improve the process parameters, especially for treatment of high concentrated mixtures (5–10% H_2S and higher), it was proposed to perform the reverse-process in two catalyst beds, placing a heat-exchanger between them to remove reaction heat and thus to increase conversion [17].

To simulate this process, the mathematical model was supported by equation of the heat-exchange. Taking the simplest model of the sulfur condenser-boiler with water cooled tubes (with production of steam), and assuming the constant wall temperature (which is generally defined by steam pressure and does not depend significantly upon other parameters) such equation may written in the following way:

$$T_{\text{out}} = \frac{T_{\text{in}} - T_{\text{w}}(1-f)}{f} \tag{52}$$

where f is dimensionless criterion, reflecting the efficiency of the heat-exchange

$$f = \exp\left(\frac{\alpha_{\text{he}} F}{W_F C_{\text{p}}}\right) \tag{53}$$

The typical results of the process simulation are shown in the Fig. 12. It is seen that the temperature profile (Fig. 12a) has the lowering in the central part of the bed, connected with intermediate gas cooling. In this case sulfur may condense at the ends of both catalyst beds (Fig. 12b). The removal of heat and sulfur provides significant gain of the conversion in the second part of the bed, providing high conversion of the initial mixture.

Fig. 13 shows the comparative conversion data for two-stage reverse-process and two-stage steady-state process. It is seen, that reverse-process provides higher sulfur removal efficiency in the area of medium and high concentration of H_2S, though the reverse-process does not comprise the gas heaters thus being cheaper and less energy consuming.

3.4. Comparison with experimental data

Reverse-flow regime was experimentally tested at the two-bed pilot reverse-flow unit with heat removal between the catalysts beds. Gas loading capacity of the unit was approximately 5000 st. $m^3\,h^{-1}$. The inlet gas contained 5–6 vol.% of H_2S and 2–3 vol.% SO_2 with moisture content of 20–25 vol.%, inlet gas temperature was ~125 °C.

The calculated and experimentally observed temperature profiles in the stabilised cycling regime (after 10 flow reversals) are shown at Fig. 14. Satisfactory coincidence between calculated and experimental data may be seen for the second catalyst bed. In the first bed the observed temperatures were higher than calculated ones. This fact is explained by the presence of oxygen in inlet gases interacting with H_2S in

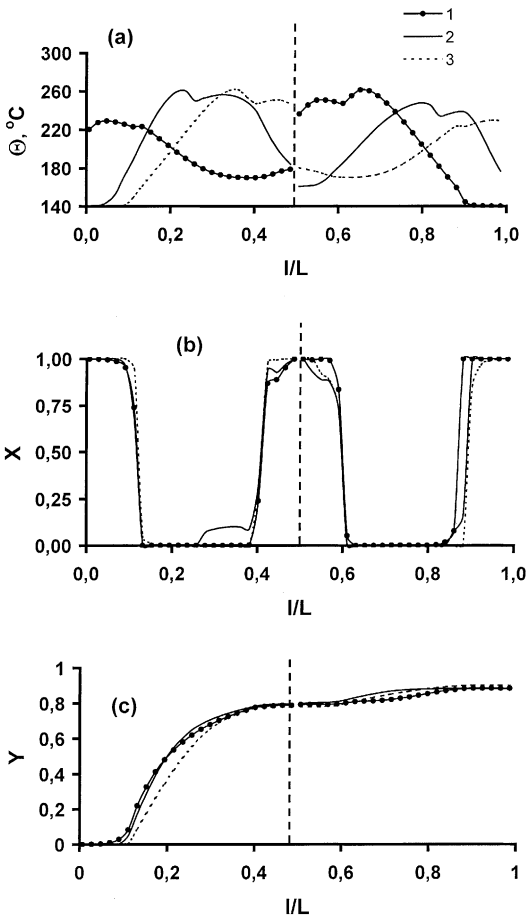

Fig. 12. Established unsteady-state regime in the two-stage Claus reverse-process: profiles of catalyst temperature (a), liquid sulfur content (b), and conversion (c) vs. bed length. Curves, 1–3, the beginning, middle and end of the cycle, respectively. Heat-exchanger parameters: heat-exchange factor $f = 3.0$, wall temperature $T_{\text{W}} = 150\,^{\circ}\text{C}$. Cycle duration $\tau_{\text{c}} = 1000$ s. Vertical dashed line shows the position of a heat-exchanger.

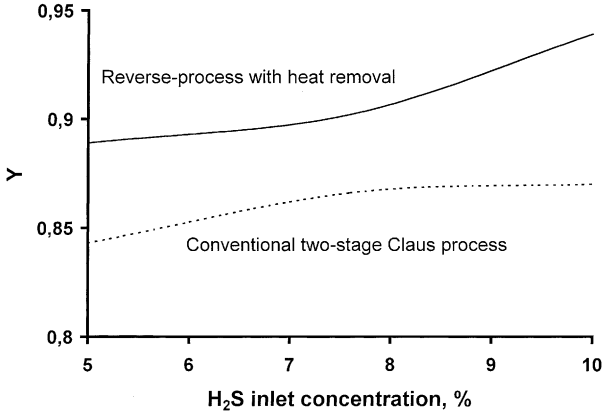

Fig. 13. Hydrogen sulphide conversion vs. inlet concentration of H_2S for two-stage processes (in vol.%). Sulfur recovery in Claus furnace is not taken into account.

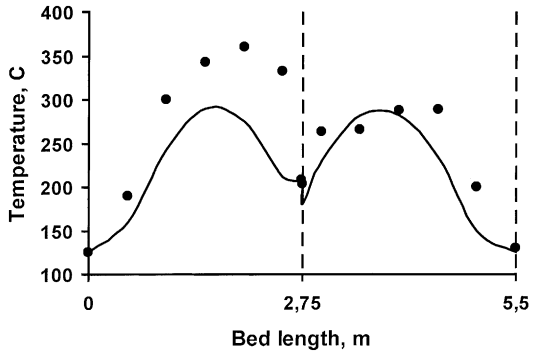

Fig. 14. Temperature profiles in the reverse-process two-bed pilot unit with intermediate heat removal. Solid lines, calculations; points, experimental data. $f = 2.6$.

this bed and leading to much higher reaction heat emission than it was proposed in simulation.

The observed H_2S conversion degree during given cycle was ~80% and that was in good agreement with simulation data, taking into account the non-optimal composition of real gases (H_2S/SO_2 ratio was visibly below 2 at the moment of measurements).

3.5. The Claus double reverse-process

The further improvement of sulfur recovery in the family of Claus reverse-processes may be achieved by the double reverse-process [17–19]. The flow-sheet of the process is presented in Fig. 15. In this process the flow reversals are performed in two technological cycles: in the internal one (in the middle reactor) and in the external one (whole installation). The middle reactor operates under low inlet temperature in the usual reverse-flow regime, providing continuous operation. The inlet bed works under high inlet temperature (300–400 °C, necessary to provide the hydrolysis of COS and CS_2, which may be present in the reaction gas), while outlet bed operates in the 'Cold Bed Adsorption' regime, providing high final conversion and adsorption of the sulfur mist formed in the condenser. Periodical flow reversals in the external cycles are made to change the outlet bed for the inlet one and vice versa. It is necessary for regeneration of the bed, filled by liquid sulfur.

Simulation results for the double reverse-process shows that the process provides high level of sulfur recovery (higher than 99%), equal to the system, comprising conventional Claus plant with tail gas cleanup unit (e.g. Sulfreen process [6,9]). At the same time the double reverse-process is characterised by much lower capital costs and energy consumption.

3.6. The 'Ring' flow-sheet

Nevertheless, the double reverse-process has the disadvantage, connected with temporary decrease of conversion degree in the beginning of each external cycle, caused by high temperature in the outlet bed in this period. In general, such period of outlet bed cooling does not take more than a few percents of total external cycle duration and the average sulfur recovery degree remains high, but that may be a problem for a large-scale plants, where even the relatively short decrease of purification efficiency is not allowed.

These problems may be solved by application of the 'Ring' Claus process [39]. In contrast to the described

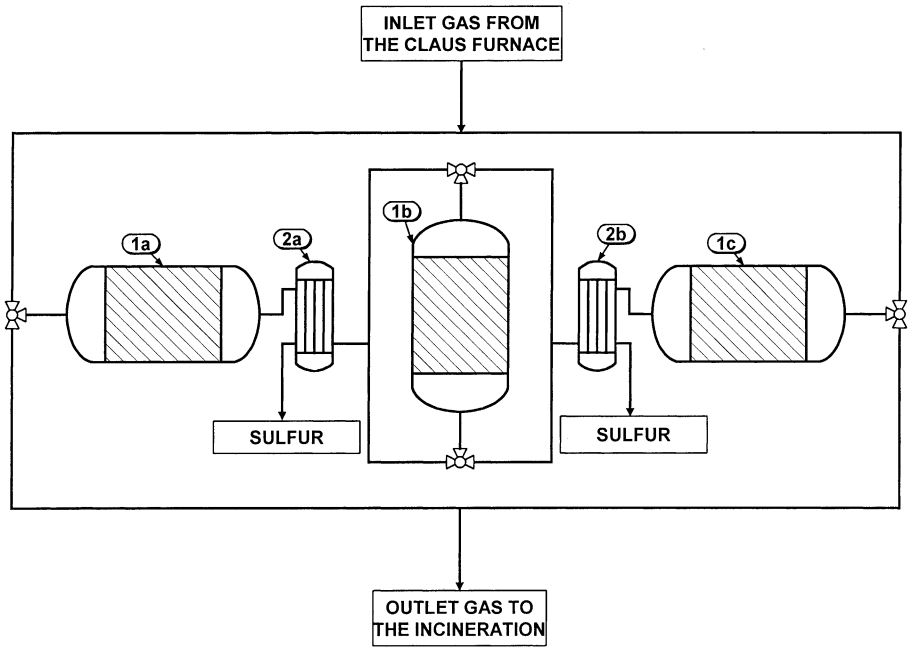

Fig. 15. Flow-sheet of the Claus double reverse-process. 1a–c, catalyst beds; 2a–c, sulfur condensers.

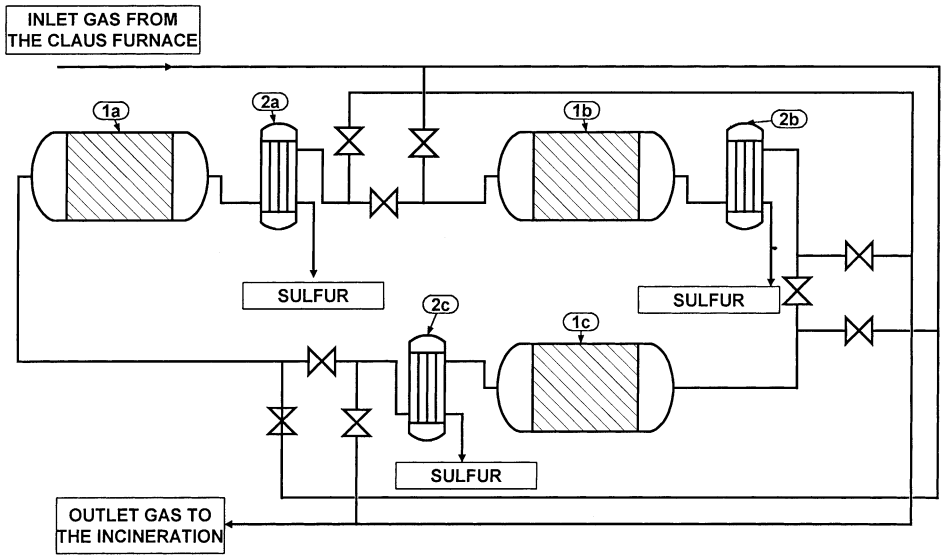

Fig. 16. Flow-sheet of the 'Ring' Claus process. 1a–c, catalyst beds; 2a–c, sulfur condensers.

above processes, the last one does not apply the reverse-flow technology, though it is also unsteady-state one. The flow-sheet of the 'Ring' process is shown in Fig. 16. The inlet bed here operates under high temperatures for hydrolysis of COS and CS_2 and partial conversion of H_2S, while second and third (outlet) beds work in 'Cold Bed Adsorption' regime. The flow sequence is periodically changed in the way to provide periodical regeneration of the bed from liquid sulfur. The 'hot' bed here becomes the second in the flow sequence, so it does not have direct connection to the outlet and its cooling period does not decrease the total efficiency of the plant.

The modelling results for the 'Ring' process show that at every moment of the cycle the sequence of the reactors contains the 'hot' bed, while the outlet one is always 'cold'. Such regime provides higher than 99% level of sulfur recovery during all operation period.

4. Reverse-process feasibility

The modelling results showed that sulfur recovery processes, based on application of reverse-flow technique and artificially created unsteady-state conditions, provide higher efficiency than conventional technologies both in terms of sulfur recovery and capital/operating costs.

Economic estimations showed that application of the reverse-process provides the decrease of the cost at the same level of sulfur removal efficiency. The value of such decrease may reach 20–30% of overall plant cost. It should be noted that unsteady-state processes are characterised by lower operation costs as well, mainly due to the significant decrease of energy consumption.

References

[1] C.F. Claus, British Patent Application No. 3608, 1882.
[2] C.F. Claus, British Patent Application No. 5070, 1883.
[3] C.F. Claus, British Patent Application No. 5959, 1883.
[4] H. Baehr, H. Mengdehl, German Patent Application No. 686520, 1932.
[5] German Patent Application No. 666572, 1936.
[6] Supplement to Sulphur, Sulphur 187, 1986, 20 p.
[7] A.R. Laengrich, W.L. Cameron, Oil Gas J. 12 (1978) 158.
[8] T. McDonald, British Patent Specification No. 717026, 1952.
[9] Sulfreen. Hydrocarbon Proc. 58 (1979) 140.
[10] CBA. Hydrocarbon Proc. 63 (1984) 74.
[11] R.L. Reed, US Patent No. 4487754, 1983.
[12] J. Wieckowska, Catal. Today 24 (1995) 405.
[13] J.A. Lagas, et al., The SUPERCLAUSTM process in light of future developments, in: Proceedings of the Sulphur-95 International Conference, November 1994.
[14] J.A. Lagas, et al., Selective-oxidation catalyst improves the claus process, Oil Gas J. 10, 1988.
[15] W. Kensell, D. Leppin, Review of the H_2S direct oxidation processes, in: Proceedings of the Seventh GRI Sulfur Recovery Conference, 1995.
[16] G.K. Boreskov, Yu.Sh. Matros, A.I. Oruzheinikov, USSR Patent No. 911852, 1981.
[17] Yu.Sh. Matros, A.N. Zagoruiko, I.V. Malakhova, O.G. Eremin, UK Patent No. 2206108, 1986.
[18] Yu.Sh. Matros, A.N. Zagoruiko, in: Proceedings of the Sulphur-90 Conference, April 1990, Cancun, Mexico, British Sulphur Corp., London, 1990, p. 107.
[19] A.N. Zagoruiko, in: Proceedings of the USPC International Conference, 5–8 June 1990, Novosibirsk, USSR, VSP, Utrecht, 1990, p. 705.
[20] Yu.Sh. Matros, G.A. Bunimovich, Catal. Rev. Sci. Eng. 38 (1996) 1.
[21] M. Razzaghi, I.G.D. Lana, Catalysis on the energy scene, in: Proceedings of the Ninth Canadian Symposium on Catalysis, Vol. 19, Elsevier Science Publishers, Amsterdam, 1984, p. 221.
[22] Yu.Sh. Matros, A.N. Zagoruiko, Dokl. Akad. Nauk. 294 (1987) 1424.
[23] A.N. Zagoruiko, A.S. Noskov, V.I. Drobishevich, L.V. Yausheva, I.V. Malakhova, Yu.Sh. Matros, Theor. Found. Chem. Eng. 23 (1989) 209.

[24] Yu.Sh. Matros, Unsteady processes in catalytic reactors, Studies in surface science and catalysts, Elsevier Science Publishers, 1985, Amsterdam.
[25] Yu.Sh. Matros, Catalytic processes under unsteady-state conditions, Elsevier Science Publishers, Amsterdam, 1988.
[26] M. Razzaghi, I.G. Dalla Lana, Can. J. Chem. Eng. 62 (1984) 413.
[27] G.R. Schoofs, Hydrocarbon Proc. 64 (1985) 71.
[28] A.N. Zagoruiko, V.V. Mokrinskii, V.I. Marshneva, Yu.Sh. Matros, Kinet. Catal. 34 (1993) 1049.
[29] I.G. Dalla Lana, C.L. Liu, B.K. Cho, Proceedings of the Sixth Europe, and Forth International Symposium, Chem. React. Eng., Vol. 196, DECHEMA, 1976.
[30] H.A. El Masry, Appl. Catal. 16 (1985) 301.
[31] D.E. McGregor, I.G. Dalla Lana, C.L. Liu, A.E. Cormode, Proceedings of the Forth Europe and Second Internatoinal Symposium, Chem. React. Eng., B2 9, Elsevier Science Publishers, Amsterdam, 1972.
[32] O.A. Malinovskaya, V.S. Beskov, M.G. Slin'ko, Modelling of catalytic processes in porous pellets, Novosibirsk, Nauka, 1975, p. 265, in Russian.
[33] C. McGreavy, D.L. Cresswel, Can. J. Chem. Eng. 47 (1969) 583.
[34] A.N. Zagoruiko, Yu.Sh. Matros, Theor. Found. Chem. Eng. 28 (1994) 633.
[35] M.E. Aerov, O.M. Todes, D.A. Narinskii, Apparatus with packed granular bed, Hydraulic and heat operation fundamentals, Leningrad, Khimia, 1979, in Russian.
[36] M. Steijns, P. Mars, Ind. Eng. Chem., Prod. Res. Dev. 16 (1977) 35.
[37] V.I. Drobishevich, V.P. Il'in, Preprint No. 307, Computing centre of SB AS USSR, Novosibirsk, 1981, in Russian.
[38] J.B. Butt, E.E. Petersen, Activation, deactivation and poisoning of catalyst. Academic Press, New York, 1988, p. 495.
[39] A.N. Zagoruiko, Yu.Sh. Matros, Russian Patent No. 4905383, 1990.